



Synthesis of unsupported two-dimensional molybdenum carbide nanosheets for hydrogen evolution



William P. Mounfield III^a, Botao Huang^c, Bin Cai^{a,c}, Yang Shao-Horn^b, Yuriy Román-Leshkov^{a,*}

^a Department of Chemical Engineering, Massachusetts Institute of Technology, Cambridge, MA 02139, United States

^b Department of Mechanical Engineering, Massachusetts Institute of Technology, Cambridge, MA 02139, United States

^c Research Laboratory of Electronics, Massachusetts Institute of Technology, Cambridge, MA 02139, United States

ARTICLE INFO

Article history:

Received 27 September 2019

Received in revised form 8 November 2019

Accepted 9 November 2019

Available online 11 November 2019

Keywords:

Molybdenum carbide

Carbide

Nanosheets

Catalysis

HER

Hydrogen evolution

ABSTRACT

A method was developed for the synthesis of multi-layered and single-layered molybdenum carbide (β -Mo₂C) nanosheets through exfoliation and centrifugation of a layered oxide precursor. The single-layer materials displayed higher intrinsic activity for the hydrogen evolution reaction (59.3 ± 6 mA/mg vs 5.3 ± 2 mA/mg) compared to the multi-layered carbide nanosheets. This effect was attributed both to high surface areas and to a more reactive surface where the binding energy of *H is optimized for the HER.

© 2019 Elsevier B.V. All rights reserved.

1. Introduction

For several decades, transition metal carbides have shown great promise as catalysts for diverse energy applications [1,2]. These materials have garnered interest due to their ability to replace or lower the loading of NMs as lower cost, earth-abundant alternatives [3]. Advances in synthetic efforts have enabled the modification of physical (e.g., strain effects) and electronic properties (e.g., oxidation resistance and d-band structure) of the material by altering its morphology [4–6].

While the production of bulk scale carbides is well established [7,8], there are currently no commercially-viable methods for the facile synthesis of ultrathin, high surface area, metal-terminated and phase-pure nanosheets [6]. Traditionally, the synthesis of 2D carbide structures has necessitated complex, multi-step procedures [9,10]. Ren et al. reported growth of 2D- α -Mo₂C thin films at the surface of molten copper via chemical vapor deposition (CVD) [9] Gogotsi et al. prepared two-dimensional early transition metal carbides, MXenes, which have shown promise as materials for Li-ion storage and in electrocatalytic applications [11–13]. These studies have shown the interesting nature of 2D carbides, but their complex synthesis has limited their wide-spread use

[14]. Therefore, a facile, robust, and general method to prepare a wide range of 2D carbides is of critical importance to effectively evaluate their catalytic applications.

Recent studies have shown that molybdenum-based materials are promising HER catalysts [15,16]. In particular, Mo₂C exhibits a Pt-like electronic structure, making it a promising substitute for Pt-based catalysts. Mo₂C, among other carbides, possesses a similar hydrogen binding energy to Pt, positioning it as a potentially highly active material for HER [17]. Given that the catalytic performances are strongly correlated to their structural properties, it is anticipated that Mo₂C nanosheets with tailored electronic structure and abundant exposed active surface would favor high HER activity.

Inspired by the facile synthesis of 2D oxides [18–20], we hypothesized that a suitable layered oxide precursor could be used as a template for layered carbides, or as a single-layer precursor after exfoliation. In this work, we investigated the production of unsupported single-layer phase-pure molybdenum carbide (β -Mo₂C) nanosheets and their implementation as efficient electrocatalysts for the hydrogen evolution reaction (HER). This method is simple and robust, thus enabling the facile synthesis of 2D carbide materials for future applications in catalysis, separations and energy storage.

* Corresponding author.

E-mail address: yroman@mit.edu (Y. Román-Leshkov).

URL: <http://romangroup.mit.edu> (Y. Román-Leshkov).

2. Experimental

Layered MoO_3 nanosheets were prepared following a similar procedure (Fig. 1) to that detailed by Nicolosi and Coleman et al. [20] MoO_3 was added to isopropanol and sonicated with a horn-probe tip sonicator. The nanosheets were separated by centrifugation and labeled either as single or multi depending on their thickness. Collected nanosheets were carburized in a flow of H_2 and CH_4 . After cooling to room temperature, the materials were passivated with a 1% O_2 /99% N_2 mixture.

Powder X-ray diffraction patterns were recorded on an Bruker Advance II diffractometer. Nitrogen physisorption isotherms were measured at 77 K using a Quantachrome Instruments Quadrasorb EVO. Transmission Electron Microscopy (TEM) was performed on a JEOL 2010F operating at 200 kV. Scanning Probe Microscopy (SPM) was performed on an NT-MDT NTEGRA system. Hydrogen evolution reaction (HER) testing was conducted with a Biologic SP-300 potentiostat in an isothermal three-electrode electrochemical system in an Ar saturated 0.1 M HClO_4 aqueous electrolyte at 293 K. Further experimental details are available in the [Supporting Data](#).

3. Results and discussion

PXRD patterns shown in Fig. 2a confirmed the obtained single and multi-layered structures matched those of MoO_3 . Surface areas were determined from N_2 physisorption isotherms (Fig. 2b and d), a value for the multi-layer material of $2.6 \text{ m}^2/\text{g}$ (see Table S1) was similar to that of bulk oxides found in literature ($\sim 1 \text{ m}^2/\text{g}$) [21]. The single-layer sample featured higher surface area, $293 \text{ m}^2/\text{g}$, well above those of high-surface area oxides [21].

Fig. S1 shows the PXRD patterns of the single and multi-layer samples after carburization at 600°C . The initial carburization resulted in incomplete conversion of MoO_3 to $\beta\text{-Mo}_2\text{C}$. To synthesize phase-pure carbide materials, a new aliquot of each exfoliated precursor was carburized at 700°C . Fig. 2b shows the patterns of freshly carburized samples match the reference $\beta\text{-Mo}_2\text{C}$ pattern, and do not display reflections from other phases. The similarity of the phase-pure single-layer surface area to that of the initial biphasic material supports the observation that the sample contains a high number of single-layer sheets.

Dark-field TEM images and electron diffraction (EDF) patterns are shown in Fig. 3 for both multi- and single-layer nanosheets. The EDF pattern in the inset of Fig. 3a shows several facets, indicating the presence of grain boundaries and multiple layers. The inset of Fig. 3c shows the EDF pattern for the large single-layer $\beta\text{-Mo}_2\text{C}$ nanosheet shown in the low magnification TEM image in Fig. 3c. The EDF pattern suggests the presence of a thin single-crystal

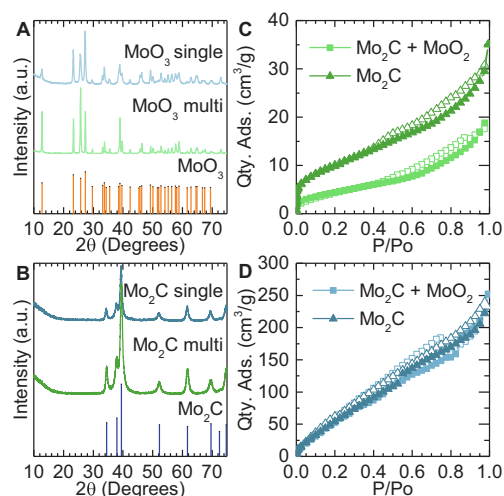


Fig. 2. (a) PXRD patterns of multi-(aqua) and single-layer (cerulean) MoO_3 nanosheets and MoO_3 JCPDS 00-005-0508 (tangerine). (b) PXRD patterns of multi-(teal) and single-layer (emerald) Mo_2C nanosheets and $\beta\text{-Mo}_2\text{C}$ JCPDS 00-011-0680 (royal blue). N_2 physisorption isotherms for (c) $\beta\text{-Mo}_2\text{C} + \text{MoO}_2$ multi-(squares) and $\beta\text{-Mo}_2\text{C}$ multi-layer (triangles) nanosheets, (d) $\beta\text{-Mo}_2\text{C} + \text{MoO}_2$ single-(squares) and $\beta\text{-Mo}_2\text{C}$ single-layer (triangles) nanosheets.

sheet, given that only the (1 0 0) reflection is visible. Fig. 3d shows a HRTEM image of a multi-layer $\beta\text{-Mo}_2\text{C}$ nanosheet with overlaid d-spacing corresponding to the (1 0 0) facet. The thicknesses of the nanosheets were confirmed with SPM of single and multi-layer nanosheets deposited on the same silicon wafer as shown in Fig. 3e,f. The theoretical height calculated for a single-layer nanosheet, $\sim 1.5 \text{ nm}$, matches that observed with SPM; other samples shown in the inset of Fig. 3e show characteristic heights for two and three-layer nanosheets from the multi-layer sample.

The as-prepared single- and multi-layer $\beta\text{-Mo}_2\text{C}$ nanosheets were evaluated as electrocatalysts for HER in an Ar-saturated (Fig. 4) and H_2 -saturated (Fig. S2) 0.1 M HClO_4 electrolyte. A graphite counterelectrode was used to avoid contamination from platinum dissolution often seen when using a platinum counterelectrode. The on-set potential was 10.7 mV for single-layer nanosheet and 24.1 mV for multi-layer sample (Fig. 4a) on the RHE scale. The single-layered $\beta\text{-Mo}_2\text{C}$ exhibits a mass activity of $59.3 \pm 6 \text{ mA}/\text{mg}_{\text{Mo}_2\text{C}}$ at $-0.2 V_{\text{RHE}}$, which is ~ 10 times higher than that of the multilayered counterparts ($5.3 \pm 2 \text{ mA}/\text{mg}_{\text{Mo}_2\text{C}}$) (Fig. 4b). Single-layered $\beta\text{-Mo}_2\text{C}$ showed comparable HER mass activity to the 1 T phase MoS_2 ($62 \text{ mA}/\text{mg}_{\text{Mo}_2\text{C}}$ at $-0.2 V_{\text{RHE}}$) [22] and polydiaminopyridine molybdenum carbonitride (PDAP-MoCN) ($48 \text{ mA}/\text{mg}_{\text{Mo}_2\text{C}}$ at $-0.2 V_{\text{RHE}}$) [23] that are higher than

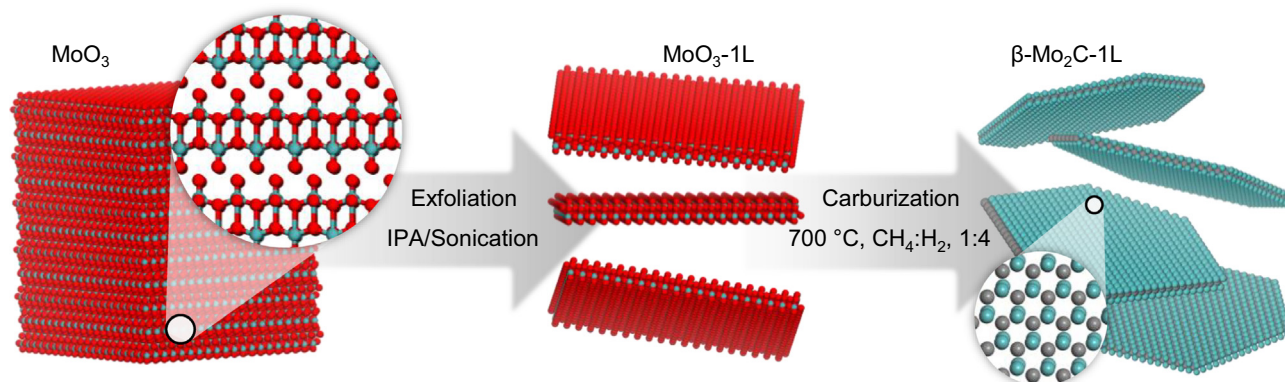


Fig. 1. Synthesis scheme for the production of $\beta\text{-Mo}_2\text{C}$ nanosheets from bulk MoO_3 through a MoO_3 nanosheet intermediate.

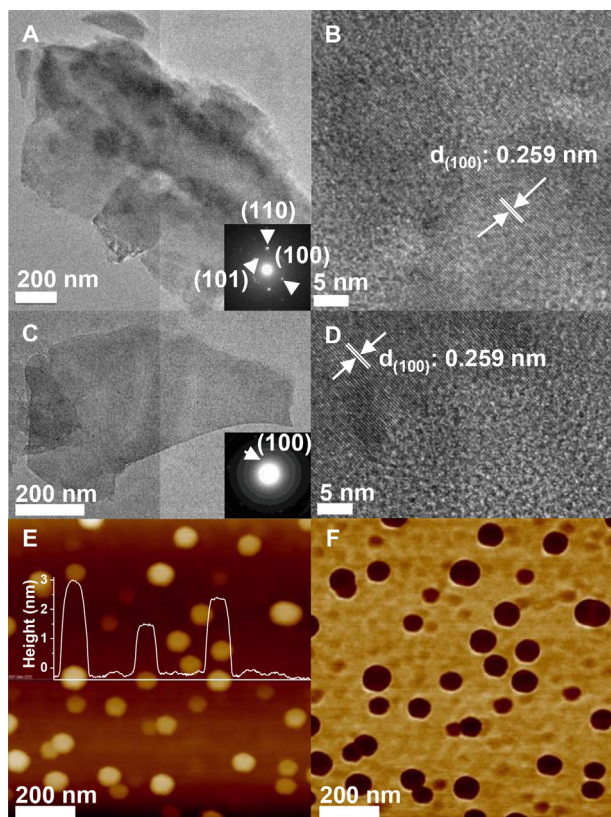


Fig. 3. TEM and HRTEM images of (a,b) multi-layer β -Mo₂C and (c,d) single-layer β -Mo₂C nanosheets. Insets of (a,c) show electron diffraction patterns for the single and multi-layer sheets. SPM height (e) and phase (f) images for single and multi-layer carbides. Inset of (e) shows the height along a linecut.

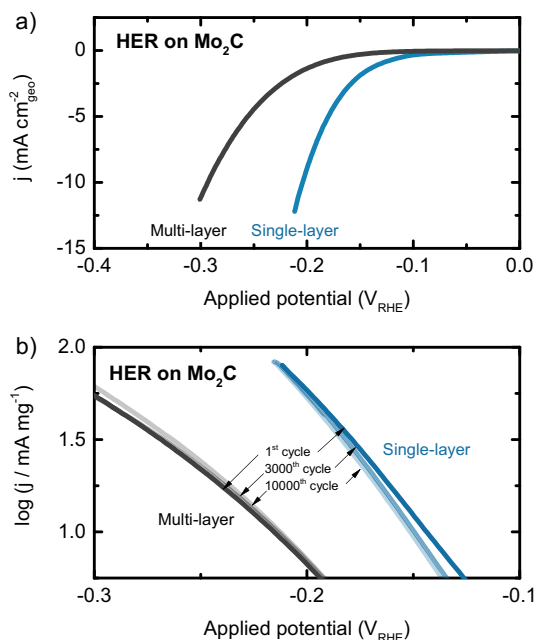


Fig. 4. HER activity on single-layer and multi-layer β -Mo₂C with catalyst loading of 30 μ g and 40 μ g, respectively, in Ar-saturated 0.1 M HClO₄ electrolyte at 1600 rpm and 20 °C. a) polarization curves. b) mass activity of catalysts at the 1st, 3000th and 10000th cycles.

those obtained for Mo₂C nanoparticles embedded on a 2D nitrogen-implanted carbon matrix (15.4 mA/mg_{Mo₂C} at -0.2 V_{RHE}) [24] and bulk MoS₂ (~ 1 mA/mg_{Mo₂C} at -0.2 V_{RHE}) [25].

Normalization by catalyst surface area (Fig. S3) showed that the increase in activity was due to a higher intrinsic activity for the single-layer nanosheets, and not solely due to an increase in the number of exposed active sites, indicating that the single-layer provides a more reactive surface for HER. Xie et al., reached similar conclusions for MoN nanosheets and determined that surface Mo atoms are the active site for the HER [26]. The higher intrinsic HER activity of the single-layer β -Mo₂C nanosheets can likely be attributed to a higher abundance of Mo-terminated sites. Further theoretical calculation is needed to determine the effect of this Mo-terminated surface on the binding energy of adsorbed hydrogen.

The Tafel slopes of both catalysts were ~ 70 mV/decade (Fig. S4), similar to those of Mo₂C nanoparticles found by Zhang et al., [24] indicating that for HER in acidic media (pH = 1) both single- and multi-layer β -Mo₂C feature a mix of Tafel/Volmer and Heyrovsky/Volmer mechanisms, with Tafel slopes of 30, 40 and 120 mV/decade for Tafel, Heyrovsky and Volmer determining rate steps, respectively [27].

Accelerated potential sweeps were conducted to assess the durability of the β -Mo₂C catalysts. Both the single and multi-layer nanosheets showed excellent stability in acidic conditions. After 10000th cycles, no significant changes were found for the mass activities at -0.2 V_{RHE} of both single- and multi-layer nanosheets (Fig. 4b).

4. Conclusion

In conclusion, the exfoliation of molybdenum trioxide was successfully used as a template for the preparation of phase-pure β -Mo₂C nanosheets of varying thicknesses. The exfoliation degree of the MoO₃ was observed to directly transfer to the thickness of β -Mo₂C nanosheets produced after carburization. Experimental analyses confirmed the presence of a more catalytically active surface for HER on single-layer nanosheets. The development of this method for the production of carbide nanosheets might serve as a reference for the design of efficient and stable carbide catalysts in 2D morphologies.

Declaration of Competing Interest

The authors declare that they have no known competing financial interests or personal relationships that could have appeared to influence the work reported in this paper.

Acknowledgments

This work is supported by the Toyota Research Institute through the Accelerated Materials Design and Discovery program, United States. The authors thank Dr. Yong Zhang and Dr. Aaron Garg for their valuable discussions and Hursh V. Sureka for assistance with SPM.

Appendix A. Supplementary data

Supplementary data to this article can be found online at <https://doi.org/10.1016/j.matlet.2019.126987>.

References

- [1] C. Kunkel et al., *Energy Environ. Sci.* 9 (2016) 141–144.
- [2] R. Michalsky et al., *ACS Catal.* 4 (2014) 1274–1278.
- [3] S.T. Hunt et al., *Energy Environ. Sci.* 9 (2016) 3290–3301.
- [4] Z. Yao et al., *RSC Adv.* 6 (2016) 19944–19951.
- [5] S.T. Hunt et al., *J. Phys. Chem. C* 119 (2015) 13691–13699.
- [6] Y. Zhong et al., *Adv. Sci.* 3 (2016), 1500286-n/a.
- [7] L. Volpe, M. Boudart, *J. Solid State Chem.* 59 (1985) 348–356.

- [8] S.T. Oyama, *Catal. Today* 15 (1992) 179–200.
- [9] C. Xu et al., *Nat. Mater.* 14 (2015) 1135.
- [10] D. Geng et al., *Adv. Mater.* 29 (2017) 1700072.
- [11] C.E. Ren et al., *ChemElectroChem* 3 (2016) 689–693.
- [12] H. Jin et al., *Chem. Rev.* 118 (2018) 6337–6408.
- [13] Z.W. Seh et al., *ACS Energy Lett.* 1 (2016) 589–594.
- [14] V.M. Hong Ng et al., *J. Mater. Chem. A* 5 (2017) 3039–3068.
- [15] H. Vrubel, X. Hu, *Angew. Chem., Int. Ed. Engl.* 51 (2012) 12703–12706.
- [16] L. Liao et al., *Energy Environ. Sci.* 7 (2014) 387–392.
- [17] Y.C. Kimmel et al., *ACS Catal.* 4 (2014) 1558–1562.
- [18] V. Nicolosi et al., *Science* (2013) 340.
- [19] B. Mendoza-Sánchez et al., *Electrochim. Acta* 174 (2015) 696–705.
- [20] D. Hanlon et al., *Chem. Mater.* 26 (2014) 1751–1763.
- [21] R. Burch, *J. Chem. Soc., Faraday Trans. 1* (74) (1978) 2982–2990.
- [22] Y. Yin et al., *J. Am. Chem. Soc.* 138 (2016) 7965–7972.
- [23] Y. Zhao et al., *J. Am. Chem. Soc.* 137 (2015) 110–113.
- [24] H. Zhang et al., *NPG Asia Mater.* 8 (2016), e293.
- [25] N. Dubouis et al., *ACS Catal.* 8 (2018) 828–836.
- [26] J. Xie et al., *Chem. Sci.* 5 (2014) 4615–4620.
- [27] T. Shinagawa et al., *Sci. Rep.-Uk* 5 (2015) 13801.